

## ANALYSIS OF GREASE CONTAMINATION INFLUENCE ON THE INTERNAL RADIAL CLEARANCE OF BALL BEARINGS BY THERMOGRAPHIC INSPECTION

by

**Žarko Z. MIŠKOVIĆ<sup>a\*</sup>, Radivoje M. MITROVIĆ<sup>a</sup>, and Zoran V. STAMENIĆ<sup>a</sup>**

<sup>a</sup> Faculty of Mechanical Engineering, University of Belgrade, Belgrade, Serbia

Original scientific paper  
DOI: 10.2298/TSCI150319083M

*One of the most important factors influencing ball bearings service life is its internal radial clearance. However, this parameter is also very complex because it depends on applied radial load and ball bearings dimensions, surface finish, and manufacturing materials. Thermal condition of ball bearings also significantly affects internal radial clearance. Despite many researches performed in order to find out relevant facts about different aspects of ball bearings thermal behaviour, only few of them are dealing with the real working conditions, where high concentration of solid contaminant particles is present. That is why the main goal of research presented in this paper was to establish statistically significant correlation between ball bearings temperatures, their working time, and concentration of contaminant particles in their grease. Because of especially difficult working conditions, the typical conveyor idlers bearings were selected as representative test samples and appropriate solid particles from open pit coal mines were used as artificial contaminants. Applied experimental methodology included thermographic inspection, as well as usage of custom designed test rig for ball bearings service life testing. Finally, by obtained experimental data processing in advanced software, statistically significant mathematical correlation between mentioned bearings characteristics was determined and applied in commonly used internal radial clearance equation. That is the most important contribution of performed research – the new equation and methodology for ball bearings internal clearance determination which could be used for eventual improvement of existing bearings service life equations.*

Key words: *radial ball bearings, internal radial clearance, contamination, thermographic inspection*

### Introduction

Rolling bearings are indisputably one of the most widely used machine elements. Nowadays they are built in almost all machines with rotary parts. According to [1] in the year of 2011<sup>th</sup>, there were already over 150000 different types of rolling bearings were used worldwide. Among them, the largest number refers to the radial ball bearings, usually consisted of inner and outer ring, balls (rolling elements), and cage.

Taking into account previously listed facts, it is clear that any improvement of radial ball bearings reliability and efficiency inevitably leads to significant savings, both financial and energetic.

---

\* Corresponding author; e-mail: zmiskovic@mas.bg.ac.rs

### Theoretical and experimental background

Relations between grease contamination level and operating parameters of the radial ball bearings are rather complex. The damage of the contact surfaces caused by contamination particles induces the bearing's radial clearance change. Also, load distribution between balls and rings of the contaminated rolling bearing is disturbed, which also affects the bearings heat generation as well as bearings vibrations intensity level [2, 3]. Furthermore, level of damage of the bearings contact surfaces depends on the hardness of the ductile contamination particles and the toughness of the brittle contamination particles, because they could be either deformed or fractured when they enter the zone between balls and rings of the contaminated bearing [4].

Ball bearings internal radial clearance could be divided into four different types (fig. 1 [5]):

- (1) theoretical internal clearance – radial internal clearance which equals measured clearance minus the elastic deformation caused by the measuring load,
- (2) residual internal clearance – clearance left in a bearing after mounting on a shaft and in a housing. The elastic deformation caused by the mass of the shaft *etc.* is usually fully neglected,
- (3) effective internal clearance – radial clearance that exists in a bearing at its operating temperature (the elastic deformation caused by load is not included), and
- (4) operating clearance – actual clearance when a rolling bearing is installed and running under a load. It includes effect of elastic deformation as well as fitting and temperature. Generally the operating clearance is not used in calculations.

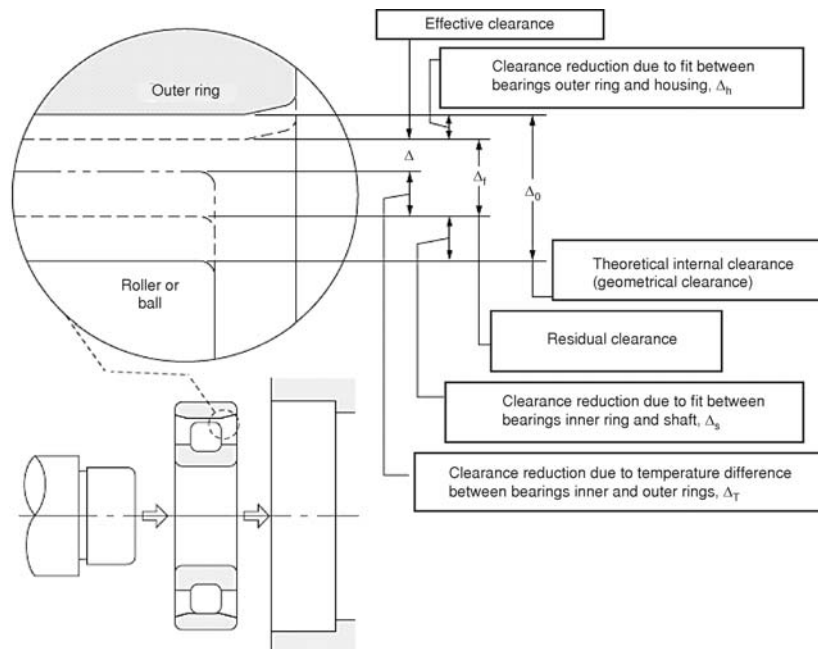


Figure 1. Graphical presentation of rolling bearings internal radial clearance types [5]

As described by Harris [6] and presented by Ricci [7], the increase in  $d_i$  due a press fitting between a bearing inner ring and a shaft of diameter  $d_2$  is calculated:

$$\Delta_s = \frac{\frac{2Id_i}{d_b}}{\left[ \left( \frac{d_i}{d_b} \right)^2 - 1 \right] \left\{ \frac{\left( \frac{d_i}{d_b} \right)^2 + 1}{\left( \frac{d_i}{d_b} \right)^2 - 1} + \nu_b + \frac{E_b}{E_s} \left[ \frac{\left( \frac{d_b}{d_2} \right)^2 + 1}{\left( \frac{d_b}{d_2} \right)^2 - 1} - \nu_s \right] \right\}} \quad (1)$$

Following the same principle, the decrease in  $d_o$  due a press fitting between a bearing outer ring and a housing hole diameter  $d_1$  could be calculated according to:

$$\Delta_h = \frac{\frac{2Id_a}{d_o}}{\left[ \left( \frac{d_a}{d_o} \right)^2 - 1 \right] \left\{ \frac{\left( \frac{d_a}{d_o} \right)^2 + 1}{\left( \frac{d_a}{d_o} \right)^2 - 1} - \nu_b + \frac{E_b}{E_h} \left[ \frac{\left( \frac{d_1}{d_a} \right)^2 + 1}{\left( \frac{d_1}{d_a} \right)^2 - 1} + \nu_h \right] \right\}} \quad (2)$$

If bearings outer and inner rings are, respectively, at temperatures  $T_o$  and  $T_i$ , and environment temperature is marked with  $T_a$ , then the radial clearance increase due to thermal expansion is:

$$\Delta_T = \Gamma_b d_o (T_o - T_a) + \Gamma_b d_i (T_i - T_a) \quad (3)$$

Last equation is valid only if both bearings rings are made from the same material – which is the most common case. If housing and shaft material is not the same as bearings, eq. (4) equals:

$$\Delta_T = (\Gamma_b - \Gamma_h) d_a (T_o - T_a) + (\Gamma_s - \Gamma_b) d_b (T_i - T_a) \quad (4)$$

Finally, total reduction of bearings internal radial clearance after mounting could be calculated:

$$\Delta = \Delta_T - \Delta_s - \Delta_h \quad (5)$$

It is important to mention that in following chapters, only eq. (3) is relevant as it will be complemented by appropriate expressions for  $T_i$  and  $T_o$  – generated by experimental data processing and analysis. Namely, progress in science nowadays allows very precise recording of temperature distribution on wide spectrum of objects surfaces using thermal imaging digital cameras. Rolling bearings are not exception. It could be even claimed that thermographic inspection rapidly becomes standardised methodology for rolling bearings condition monitoring [8]. However, except for monitoring purposes, mentioned methodology could be used for scientific researches in unexplored areas of bearings thermal behaviour. For example, Seo *et al.* [9] used thermographic inspection to observe rolling bearings surface temperature change in different lubricating conditions (normal condition, lubricating oil loss condition, and spalling) with variable rotational speeds of 1000 rpm, 2000 rpm, and 3000 rpm. As a test samples, they have used 6004, 6204, and 6304 radial ball bearings.

Also, available comercial softwares for finite element method are often used for simulation of heat generation and transfer in rolling bearings. Example of such a research is presented by Kushwaha *et al.* [10]. They have modeled typical radial ball bearing (type: 7206) and

its environment in order to simulate the maximum temperature in the bearing as a function of time with the rotational speed as a variable parameter (1000, 2000, 3000, and 5000 rpm). The main goal of their research was to determine how fast the temperature changes in the bearing system and if a given maximum temperature (*e. g.* maximum temperature of the lubricant or bearing metal) is reached. The simulation showed that the higher the rotational speed is, the faster the system reaches a steady-state.

Despite overall accessibility of wide range of different models of thermal imaging cameras, produced by many different manufacturers, analysis of the available literature have shown

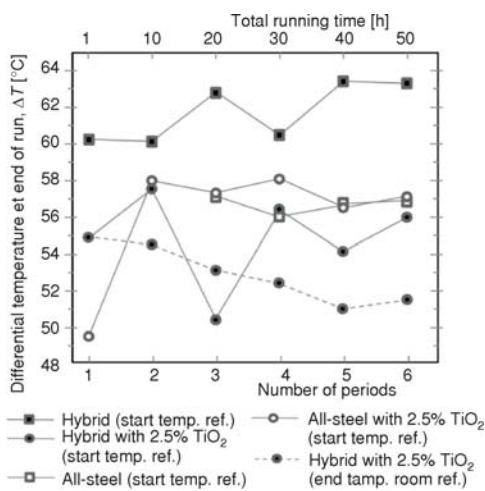


**Figure 2. Differential race temperatures measured on the upper race, with and without titania contaminant in lithium grease [11]**

that so far thermographic inspection was not used in researches dealing with the rolling bearings contaminated by solid particles. However, other methodologies for temperature measurement (such as thermocouple probes) were used – as in research performed by Kahlman and Hutchings [11]. They have tested hybrid rolling bearings, artificially contaminated by two types of contaminant particles: titania (TiO<sub>2</sub>; anatase), a relatively soft oxide with a small particle size (4 μm, mainly <1 μm); and silica (SiO<sub>2</sub>; a-quartz), a harder material with a larger particle size (75-103 μm). During the experimental testing rotational speed of tested rolling bearings was approximately 2060 rpm and some of the gained results are shown on fig. 2.

Inspired by described researches, authors of this paper have designed and performed appropriate ball bearings experimental testing, which includes thermographic inspection as well as usage of a custom made test rig.

### Experimental set-up

In this particular experimental research, working conditions of conveyor idler bearings from open pit coal mines were simulated but presented basic principles and presumptions are universal so they can be conditionally applied on any kind of rotating machinery working in hostile environments, where high concentration of debris particles is dominant, such as one described by Tasić *et al.* [12].

#### Starting assumptions

- Only the conditions of the conveyor garlands middle idler are simulated and aggravated by increased radial load and rotational speed – thus, axial loads are fully neglected and it is presumed that middle idler take 70% of total load due to weight of belt and transported material.
- In case of coal transportation, where transported material is lignite (density: 1.3 t/m<sup>3</sup>) and weight of 1 m of rubber belt is approximately 33 kg, radial load acting on the middle conveyor idler equals 3.875 kN. If radial load due to conveyor idlers rotational parts mass is added (0.165 kN, obtained by standard 3-D modelling software), it is calculated that exploitative radial load acting on each of the two conveyor idlers bearings in described conditions equals ~2.0 kN. However, in order to accelerate the bearings contact surface

damage during the experimental testing, radial load applied on tested rolling bearings was 4.6 kN.

- When the conveyor belt speed is 5 m/s, 159 mm conveyor idlers rotational speed equals approximately 600 rpm. Similar to the experimental radial load, in order to accelerate the damage of the tested conveyor idler bearings, applied experimental rotational speed (1140 rpm) was two times larger than exploitative, which leads to the conclusion that acceleration of the performed experiments was ~22.7. This means that 1 hour of bearings work in experimental conditions corresponds to 22.7 hours. of its work in exploitation – without contamination particles present;
- It is considered that mass of grease in the conveyor idlers bearings does not decrease during the exploitation and that contamination particles coming from the environment to the internal areas of the bearings are evenly distributed in their grease.
- All thermal resistances in heat transfer between inner and outer bearings raceways and its rings surfaces are neglected (sample bearings are made from good heat conductor – steel).

#### Ball bearings and grease test samples

Basic characteristics of 6310-2Z/C3 radial ball bearings, chosen for experimental testing because they are the most common bearings mounted in conveyor idlers with outer diameters of 159 mm, are presented in tab. 1. Masses of all test samples (70 in total) were measured and after ultrasonic cleaning measured again in order to determine the average weight of grease inside them (the result was 9.3 g). Among those samples, six were selected for further testing because their internal radial clearance was the same – 30 μm (measured by accredited laboratory of Faculty of Mechanical Engineering, University of Belgrade).

**Table 1. Nominal characteristics of sample radial ball bearings [13]**

Designation	SKF 6310-2Z/C3
Inner diameter, $d$	50 mm
Outer diameter, $D$	110 mm
Width, $B$	27 mm
Dynamic load capacity, $C$	65 kN
Static load capacity, $C_0$	38 kN
Reference speed	13000 rpm

Selected bearings were then regreased with pre-contaminated grease, prepared for thermographic inspection by painting of their inner and outer rings with black paint (emissivity  $\varepsilon = 0.93$ ) and exposed to the previously determined experimental radial load and rotational speed.

**Table 2. Nominal characteristics of grease used in experiment [13]**

Designation	SKF LGWA 2
DIN 51825 code	KP2N-30
NLGI consistency class	2
Soap type	Lithium complex
Base oil type	Mineral
Operating temperature range	-30 to +140 °C (-20 to +285 °F)
Base oil viscosity 40 °C, mm <sup>2</sup> /s	185
100 °C, mm <sup>2</sup> /s	15

Because of its high endurance, the SKF LGWA 2 grease was chosen for pre-contamination. Characteristics of that grease are presented in tab. 2. In total, three grease samples were prepared:

- (1) clean grease (in packages of 9.3 g),
- (2) grease with 10,75% of contaminant particles (in packages of 9.3 g of clean grease + 1 g of contamination particles), and
- (3) grease with 21.5% of contaminant particles (in packages of 9.3 g of clean grease + 2 g of contamination particles).

### Experimental contamination particles

First step in preparation of the contamination particles relevant for planned experiments was to analyse structure and size of particles present on open pit coal mines: surface dust, excavation dirt and coal dust.

After that, fifteen failed idlers were taken from the open pit coal mine conveyor and disassembled. Contamination particles from their bearings were then extracted, analysed and compared with the previous results, pointing out that typical cause of conveyor idler bearings failure was the excavation dirt, shown on fig. 3 (not the surface dust, as expected), mostly consisted of different kinds of quartz and fematite and magnetite.

At last, artificial bearing contaminant was prepared by excavation dirt sieving with appropriate mechanical screen (screen mesh size was smaller than  $120\ \mu\text{m}$  – in accordance with similar researches performed by other authors [10]).

### Testing equipment

For applying of the predefined radial load and rotational speed on tested radial ball bearings the custom made test rig was used, fig. 4(a). In order to perform planned thermographic measurements test rig was reconstructed in a way that will provide optical visibility of tested bearings inner and outer rings, fig. 4(b). Also, one of advantages of reconstructed test rig was its ability to provide accurate testing of two rolling bearings at the same time.

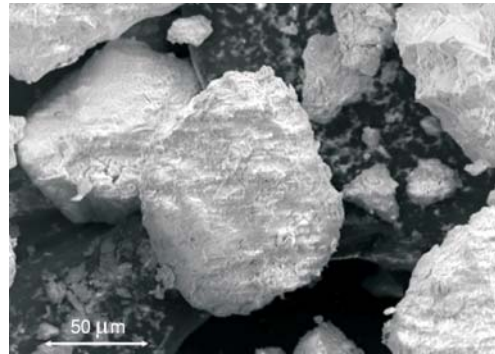


Figure 3. The SEM image of the open pit coal mine excavation dirt particles (used as an artificial contaminant in performed experimental research)

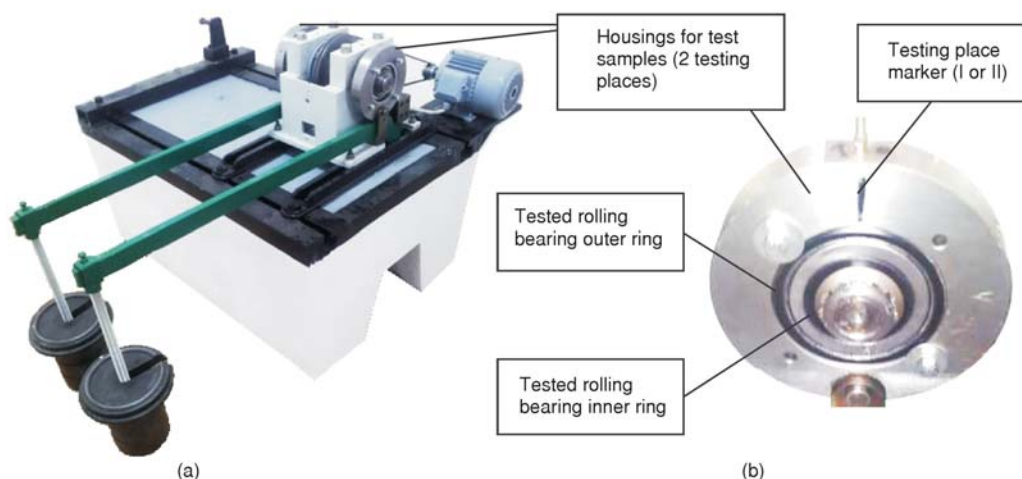


Figure 4. (a) Custom made test rig for rolling bearings service life testing, (b) Optical visibility of tested rolling bearings rings

Rolling bearings rings surface temperature distribution was recorded using advanced digital thermal camera IRC57 InfraCAM SD, manufactured by FLIR Co., USA, with temperature measurement range of 10-350 °C, and  $\pm 2\%$  accuracy [14]. Example of obtained thermal images is shown on fig. 5.

#### Testing procedure

All six selected samples (6310-2Z/C3 ball bearings with internal radial clearance of 30  $\mu\text{m}$ ) were tested in pairs on described test rig, in controlled environmental conditions (ambient temperature:  $\sim 20^\circ\text{C}$ ), according to the following procedure:

- (1) first pair of samples was greased by 9.3 g of clean grease (per sample),
- (2) second pair of samples was greased by 9.3 g of grease contaminated by 1 g of prepared particles (per sample),
- (3) third pair of samples was greased by 9.3 g of grease contaminated by 2 g of prepared particles (per sample),
- (4) first pair of samples was mounted on the test rig and exposed to radial load of 4.6 kN and rotational speed of 1140 rpm,
- (5) every ten minutes surface temperature field of sample bearings was recorded,
- (6) after 10 hours of testing experiment was finished and sample bearings were dismantled from the test rig,
- (7) second pair of samples was mounted on the test rig and exposed to radial load of 4.6 kN and rotational speed of 1140 rpm,
- (8) every ten minutes surface temperature field of sample bearings was recorded,
- (9) after 10 hours of testing experiment was finished and sample bearings were dismantled from the test rig,
- (10) third pair of samples was mounted on the test rig and exposed to radial load of 4.6 kN and rotational speed of 1140 rpm,
- (11) every ten minutes surface temperature field of sample bearings was recorded, and
- (12) after 10 hours of testing experiment was finished and sample bearings were dismantled from the test rig.

#### Experimental results

As it is not clearly defined in eq. (3) whether  $T_i$  and  $T_o$  are average or maximal temperatures of bearings inner and outer rings, it is adopted that for further analysis only the highest measured temperatures are relevant, because they are located closest to the bearings rings contacts with rolling elements – exactly where internal radial clearance is measured. Those temperatures are obtained by thermal images analysis (in total, 378 thermal images), performed in publicly available licence free software FLIR quickreport version 1.2 SP2, as in example presented in fig. 6.

Graphical presentation of measured inner and outer bearings rings surface temperatures change in time is shown on figs. 7(a) and 7(b), respectively.

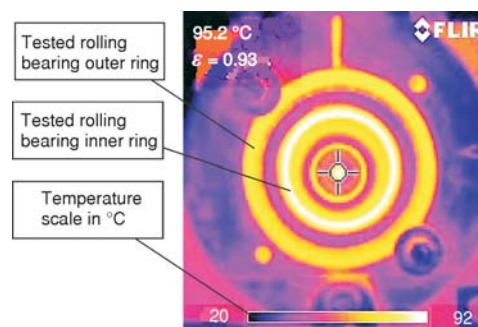


Figure 5. Example of recorded rolling bearings inner and outer rings surface temperatures

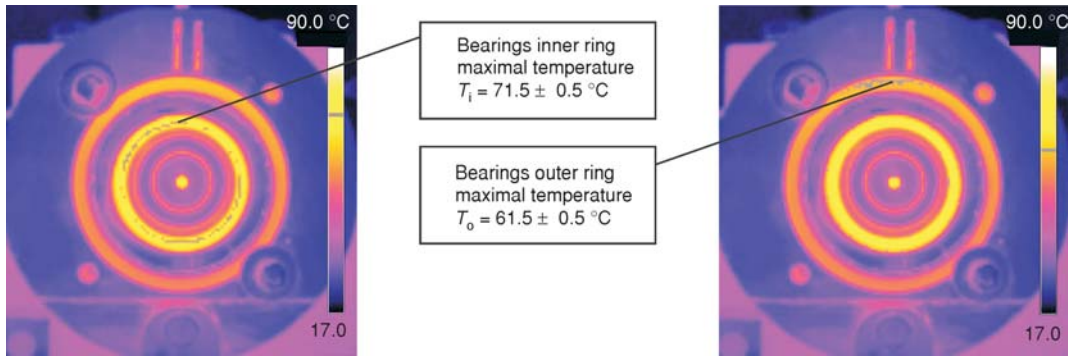


Figure 6. Maximal temperatures of sample bearings inner and outer rings

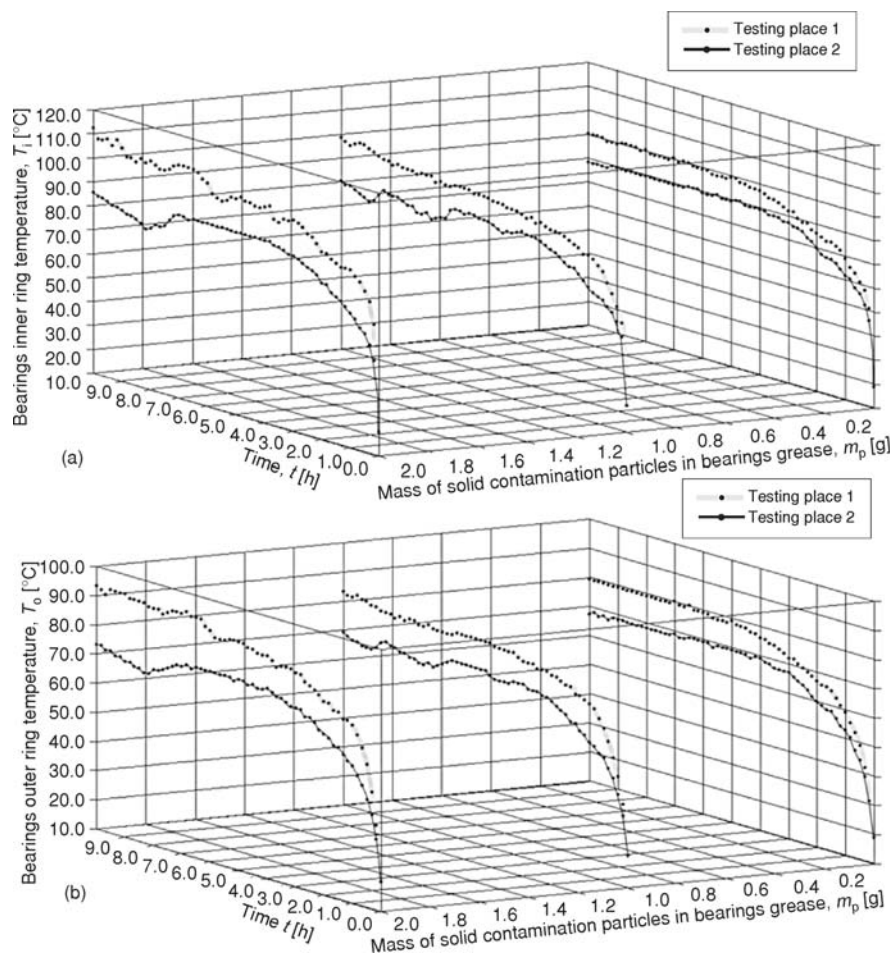


Figure 7. (a) Measured temperatures change in time of sample bearings inner rings ( $T_i$ ), (b) Measured temperatures change in time of sample bearings outer rings ( $T_o$ )

**Mathematical models**

Using software for statistical analysis and data interpolation, over 250 different interpolation models were implemented on measured experimental values, and the most relevant regarding to its statistical significance (both for bearings inner and outer rings temperatures) was:

$$T_x = a + bt + ct^2 + dt^3 + et^4 + ft^5 + gm_p + hm_p^2 \tag{6}$$

In eq. (6), variable  $T_x$  could be  $T_i$  or  $T_o$ , respectively, and coefficients  $a, b, c, d, e, f, g,$  or  $h$  depends on demanded confidence intervals – their values for described specific experimental conditions and confidence interval of 95% are given in tab. 3 (as a sample one of obtained correlations is graphically presented on fig. 8).

**Table 3. Generated mathematical models coefficients  $a, b, c, d, e, f, g,$  and  $h$  for 95% confidence interval**

Variable	$T_i$ testing place 1	$T_o$ testing place 1	$T_i$ testing place 2	$T_o$ testing place 2	$T_i$ average	$T_o$ average
$a$	33.38664	23.54225	33.00686	24.72513	33.19700	24.13369
$b$	54.34828	52.45724	41.90972	38.72921	48.12900	45.59323
$c$	-23.56598	-21.77906	-15.95475	-14.44643	-19.76000	-18.11274
$d$	4.89103	4.37554	3.09055	2.75029	3.99100	3.56291
$e$	-0.47126	-0.41213	-0.29390	-0.25741	-0.38300	-0.33477
$f$	0.01697	0.01458	0.01073	0.00926	0.01400	0.01192
$g$	1.79508	-0.15574	-1.09836	-1.47541	0.34800	-0.81557
$h$	2.63115	2.76230	1.70492	1.83607	2.16800	2.29918

It is also important to mention that coefficients of multiple determination ( $R^2$ ) for obtained correlations equals 0.696 and 0.755 (for  $T_i$  and  $T_o$ , respectively), which are the highest gained values for all tested interpolation models.

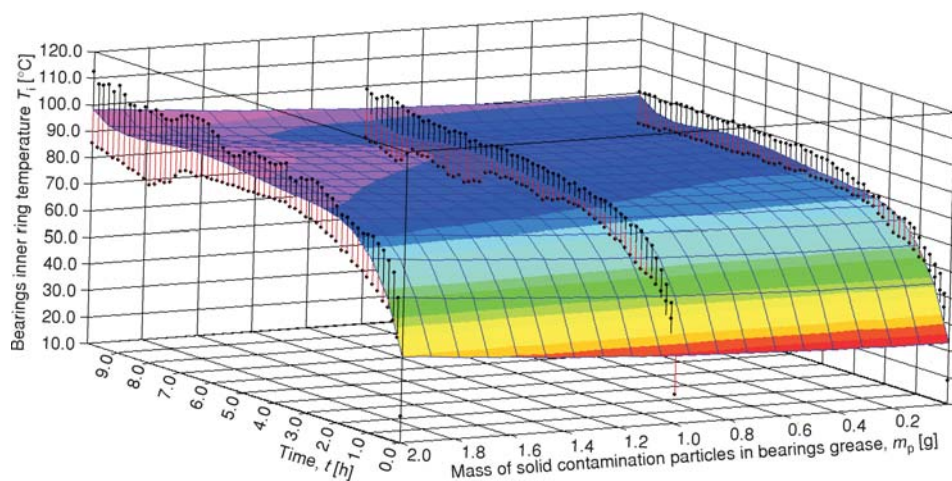


**Figure 8. Graphical presentation of generated correlation between tested radial ball bearings inner rings temperatures, time, and mass of solid contamination particles in their grease**

## Results discussion and implementation

As expected, the highest temperatures of bearings outer rings surfaces were concentrated on small areas closest to the contacts with their rolling elements, while highest temperatures of bearings inner rings surfaces were spread across their circumferences (fig. 6), which is caused by the fact that during the testing rolling bearings inner rings were rotating while the outer rings were fixed in the housings.

Analysis of the experimental results presented in fig. 7 has shown significant difference in measured bearings surface temperatures in two testing places. This could be explained by small differences in testing places housings dimensions, despite the fact that all relevant fits were within permitted boundaries. Also, tested rolling bearings mounting conditions were slightly different, which could not be avoided as it is caused by test rig construction characteristics.

During the testing, sample bearings measured surface temperatures were very consistent – bearings tested in the same experimental conditions have shown almost identical thermal behaviour. All of the samples have reached thermal balance after 3-4 hours, with visible direct correlation between mass of solid contamination particles in tested bearings grease and increment of the bearings temperatures (for example, for clean grease maximal inner and outer rings temperature increments were, respectively, 70 °C and 60 °C; for grease with 1 g of contamination particles, 78 °C and 61 °C; for grease with 2 g of contamination particles, 93 °C and 75 °C). It is also interesting to notice that in all tested samples, inner rings temperatures were higher than one in outer rings, which could be explained by less convenient load distribution due to inner rings smaller diameters.

Regarding to the generated mathematical correlations, it could be considered that gained coefficients of multiple determination are relatively high (>0.5), which leads to the conclusion that they represent measured values with reasonable accuracy so they could be replaced in eq. (3).

Finally, new equation for calculation of the internal radial clearance increment due to thermal expansion, valid for described experimental conditions, is:

$$\begin{aligned} \Delta_T = & \Gamma_b d_o (24.134 + 45.593t - 18.113t^2 + 3.563t^3 - 0.335t^4 + 1.192t^5 - \\ & - 0.816m_p + 2.299m_p^2 - T_a) + \Gamma_b d_i (33.197 + 48.129t - 19.760t^2 + 3.991t^3 - \\ & - 0.383et^4 + 1.385t^5 + 0.348m_p + 2.168m_p^2 - T_a) \end{aligned} \quad (7)$$

## Conclusions

Taking into account total number of tested bearing samples it could not be fully claimed that developed mathematical models are perfect – however, at the moment they are unique, so they could be successfully used as a basis for further researches. For example, rolling bearings service life equation (from actual standard ISO 281:2007) could be additionally improved, because at the moment it totally neglects very significant influence of bearings internal radial clearance.

## Acknowledgment

Research presented in this paper was realised within Projects TR35029 and TR14033, so authors would like to express their sincere gratitude for material and financial support to the Ministry of Education, Science and Technological Development of the Republic of Serbia.

## Nomenclature

$d_a$	– bearing outer diameter, [m]	$I$	– diametral interference, [m]
$d_b$	– bearing inner diameter, [m]	$t$	– time, [h]
$d_o, d_i$	– bearing outer and inner race diameter, [m]	$\nu_b, \nu_s, \nu_h$	– bearing, shaft, and housing Poisson's ratio, [-]
$E_b, E_s, E_h$	– bearing, shaft, and housing modulus of elasticity, [Nm <sup>-2</sup> ]	<i>Greek symbols</i>	
$m_p$	– mass of solid contamination particles in bearings grease, [g]	$\Gamma_b, \Gamma_s, \Gamma_h$	– bearing, shaft, and housing coefficient of linear expansion, [mm <sup>-1</sup> °C <sup>-1</sup> ]

## References

- [1] \*\*\*, U.S. Department of Commerce – National Security Assessment of the Ball and Roller Bearing Industry, [https://www.bis.doc.gov/index.php/forms-documents/doc\\_view/59-statistical-handbook-of-the-ball-and-roller-bearing-industry-update-2014](https://www.bis.doc.gov/index.php/forms-documents/doc_view/59-statistical-handbook-of-the-ball-and-roller-bearing-industry-update-2014)
- [2] Tomovic, R., Calculation of the Necessary Level of External Radial Load for Inner Ring Support on q Rolling Elements in a Radial Bearing with Internal Radial Clearance, *International Journal of Mechanical Sciences*, 60 (2012), 1, pp. 23-33
- [3] Mitrović, R., Study on Influence of Design and Tribology Parameters on Rolling Bearings Working Performances during High Speed Rotations, Ph. D. thesis, Faculty of Mechanical Engineering, University of Belgrade, Belgrade, 1992
- [4] Dwyer-Joyce, R. S., Predicting the Abrasive Wear of Ball Bearings by Lubricant Debris, *Wear*, 233-235 (1999), pp. 692-701, doi:10.1016/S0043-1648(99)00184-2
- [5] \*\*\*, NSK – Internal Clearance – Types and Norms, [http://www.nskeurope.com/cps/rde/dtr/eu\\_en/literature\\_bearing/TI-EN-0110-FINAL.pdf](http://www.nskeurope.com/cps/rde/dtr/eu_en/literature_bearing/TI-EN-0110-FINAL.pdf)
- [6] Harris, T., Rolling Bearing Analysis, John Wiley and Sons Inc., New York, USA, 2001
- [7] Ricci, M., Internal Loading Distribution in Statically Loaded Ball Bearings Subjected to a Combined Radial, Thrust, and Moment Load, Including the Effects of Temperature and Fit, *Proceedings*, 11<sup>th</sup> Pan-American Congress of Applied Mechanics, Foz do Iguaçu, Brazil, 2010, pp. 1-6
- [8] Bakić, G., et al., New Methodology for Monitoring and Prevention of Rotating Parts Failures, *FME Transactions*, 35 (2007), 4, pp. 195-200
- [9] Seo, J., et al., Quantitative Assessment of the Detection of Defects by Thermographic Inspection in Vibration Machinery Mode, *Proceedings*, 18<sup>th</sup> International Conference on Composite Materials, Jeju Island, South Korea, 2011, pp. 1-4
- [10] Kushwaha, A., et al., Analysis of the Ball Bearing Considering the Thermal (Temperature) and Friction Effects, *International Journal of Engineering Research and Applications (IJERA)*, Special issue (2012), 21, pp. 115-120
- [11] Kahlman, L., Hutchings, I., Effect of Particulate Contamination in Grease-Lubricated Hybrid Rolling Bearings, *Tribology Transactions*, 42 (1999), 4, pp. 842-850
- [12] Tasić, M., et al., Influence of Running Conditions on Resonant Oscillations in Fresh-Air Ventilator Blades used in Thermal Power Plants, *Thermal Science*, 13 (2009), 1, pp. 139-146
- [13] \*\*\*, SKF, <http://www.skf.com/group/splash/index.html>
- [14] \*\*\*, Exttech IRC57 InfraCam SD Thermal Imaging Camera, <http://www.instrumentation2000.com/>